34th AIAA Fluid Dynamics Conference and Exhibit
June 28–July 1, 2004/Portland, OR

Development of a Flexible Framework for Hypersonic Navier-Stokes Shuttle Orbiter Meshes

Stephen J. Alter*
NASA Langley Research Center Hampton, Virginia 23681-2199

James J. Reuther †and Ryan D. McDaniel†
NASA Ames Research Center Moffett Field, California 94035

A flexible framework constructing block structured volume grids for hypersonic Navier-Stokes flow simulations was developed for the analysis of the Shuttle Orbiter Columbia. The development of the framework, which was partially based on the requirements of the primary flow solvers used, resulted in an ability to directly correlate solutions contributed by participating groups on a common surface mesh. A foundation was built through the assessment of differences between different solvers, which provided confidence for independent assessment of other damage scenarios by team members. The framework draws on the experience of NASA Langley and NASA Ames Research Centers in structured grid generation, and consists of a grid generation process implemented through a division of responsibilities. The nominal division of labor consisted of NASA Johnson Space Center coordinating the damage scenarios to be analyzed by the Aerothermodynamics Columbia Accident Investigation (ACAI) team, Ames developing the surface grids that described the computational volume about the Orbiter, and Langley improving grid quality of Ames generated data and constructing the final computational volume grids. Distributing the work among the participants in the ACAI team resulted in significantly less time required to construct complete meshes than possible by any individual participant. The approach demonstrated that the One-NASA grid generation team could sustain the demand of for five new meshes to explore new damage scenarios within an aggressive time-line.

I. Nomenclature

$\nabla^2\vec{r}$	Stretching factor between neighboring cells
ϕ	Deviation angle from the wall unit normal to the grid that intersects a wall
σ	Standard deviation
θ	Grid line intersection angle
Θ	Grid line straightness from the body to the outer boundary
ξ,i	Streamwise computational direction and index measured from nose to tail of body
η,j	Circumferential computational direction and index from top to bottom of body

*Senior Aerospace Engineer, Senior Member AIAA
†Aerospace Engineer, Member AIAA
This material is declared a work of the U.S. Government and is not subject to copyright protection in the United States.2004

ζ,k	Computational direction and index normal to body
$\vec{r}_{\xi,\eta,\zeta}$	First derivative of Cartesian coordinates with respect to either ξ, η, or ζ
X, Y, Z	Cartesian coordinates

II. Introduction

On Sunday February 1st, 2003, Space Shuttle Orbiter Columbia performing the Shuttle Transportation System mission 107 (STS-107), disintegrated during Earth re-entry. In response, the Columbia Accident Investigation (CAI) team was formed by NASA. Within the CAI team, the Aerothermodynamic CAI (ACAI) team investigated the role of hypersonic surface heat transfer on the demise of the Shuttle Orbiter. The flow simulation software used to assess viscous hypersonic flow fields requires the use of block structured grids. These grids are difficult to generate because of the geometric complexity of the flow field, the vehicle shape, and different mesh quality and mesh topology demands of the various flow simulation codes.

This paper lays out the process that evolved into a flexible framework for the development of a common structured grid model of the Space Shuttle Orbiter, needed by the ACAI. The cooperation among ACAI team members led to efficient grid generation through the separation of steps throughout the process. The result of this framework was the generation of a family of five volume grids in the short time frame of three weeks per mesh, enabling the computational community to respond to the need for simulating viscous flow fields.

III. Grid Generation Framework

The flexible framework used by the ACAI for constructing grids consisted of a grid generation process and a division of responsibilities. Flexibility was enabled by permitting ACAI team participants to contribute at any level of the process. During the investigation, several participants performed grid quality analyses to ensure the viability of generated grids for their respective CFD tools. In order to develop a grid generation process for constructing structured grids about the Space Shuttle Orbiter, several issues required addressing:

[1] flow solvers in use;

[2] topologies and grid resolution; and

[3] grid quality.

Each issue is addressed in the following sections. Then, the process that was developed to address each issue is explained along with the rationale. Due to the fast pace of the investigation, the process chosen is very specific to the needs of the ACAI team, while not necessarily constituting the best practices of grid generation. Rather, the process is a compromise among all the issues addressed in the above list, subject to the constraints imposed by the availability of distributed grid generation resources, the need to have grid independent solution validation between flow solvers, and a very aggressive time line.

A. Flow Solvers

Prior to constructing any discrete representation of a flow field domain, the requirements for the flow solvers in question needed to be addressed. For the ACAI team, the flow solvers needed to accurately predict low density, viscous flow field phenomenon. The intended flow solvers were: the Langley Aerothermodynamic Upwind Relaxation Algorithm[1] (LAURA), the General Aerodynamic Simulation Program[2] (GASP), the Data Parallel Lower Upper Relaxation 3D (DPLUR3D) code, the Unified Solution Algorithm[3] (USA), and the Sandia Advanced Code for Compressible Aerothermodynamics Research and Analysis[4] (SACCARA). Each code has the ability to simulate the flow field phenomenon in question. However, each code has unique demands on the mesh.

For example, the DPLUR3D code requires that the block structured mesh have both face-to-face matching with no sub-facing and point-to-point matching across each block interface. The LAURA code, meanwhile can use a point-to-point, but can also have multiple cells matching a single cell on either side of the interface. Further, the LAURA code makes use of a grid adaptation scheme which requires that grid lines emanating from the outer mold line (OML) surface traverse through the flow field and map directly to the outer boundary of the flow domain.

Most flow solvers typically yield improved solution accuracy when orthogonality of the mesh to the OML is enforced. The spacing at and near the OML surface in the normal direction must be strictly enforced such that the first point off the surface is placed at a distance that is proportional to the local speed of sound. Near wall spacing and the number of points and distribution of the points within the boundary layer must meet flow solver accuracy requirements. Because some flow solver codes have difficulties with singularities, the ACAI team decided not to utilize pole boundaries in the common volume grids. Finally, grid skewness should be limited within the volume grid.

Hence, the requirements for the grids to be produced are a direct result of the chosen flow simulation software. In particular, the volume grids should be orthogonal to the wall, have minimized skewness where possible, have no singularities, and provide a point-to-point mapping from the wall to the outer boundary and block faces. By maintaining these requirements on grid construction, the full suite of flow solvers chosen should be able to provide accurate aerothermodynamic predictions of the hypersonic flow field phenomenon.

B. Topology and Grid Resolution

Structured grids are characterized by three mutually orthogonal computational coordinates, forming a rectilinear lattice of points in an ordered three-dimensional (3D) array. The vehicle's topology is created when the mesh is combined with a mapping that dictates how the points conform to the surface and surrounding volume. The mapping is the link between the physical domain where the vehicle is described with physical coordinates such as (x,y,z) in a Cartesian domain, to a computational domain where the coordinates are typically (i,j,k) and typically form a rectangular box. Because of the requirements imposed by the various flow solvers and the need to develop a common mesh that could accommodate all the methods, the choice of mesh topology, structure, and quality were limited. As such, a multiple block grid with a global O-grid topology over the vehicle was chosen, coupled with a C-grid on the tail and wing, and a region along the wing leading edge that could accommodate an embedded O-grid, as shown in figure 1.

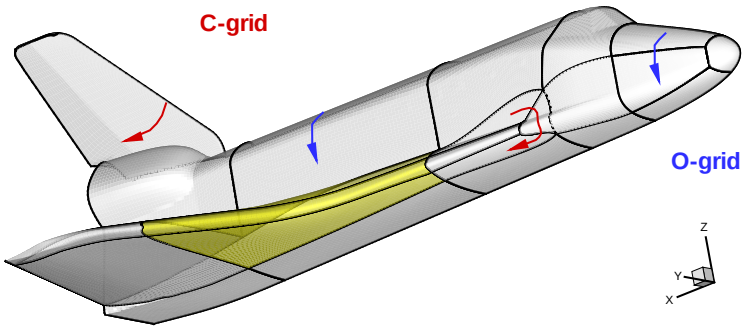

Figure 1. Shuttle Orbiter structured grid topology.

Shaded in yellow is the region of damage scenarios where the embedded O-grid could be used to isolate various types of geometry changes. The topological structures in use serve to limit the grid resolution where it is not warranted, while offering enhanced resolution were it is needed for flow solver accuracy.

There are three basic possible structured grid topologies, as shown in figure 2.

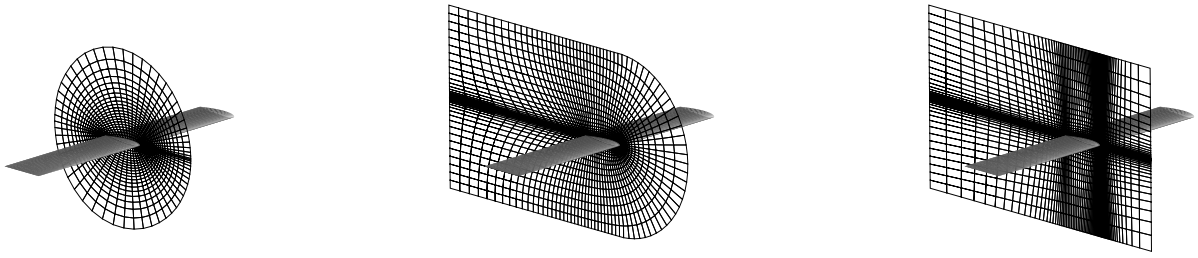

(a) O-grid. (b) C-grid. (c) H-grid.

Figure 2. Basic structured grid topologies on a wing.

Each topology is so named because of its structure; the O-grid looks like an O, and similarly for the C- and H-grids. Each topology has advantages and disadvantages. For the shuttle geometry, a full body O-grid is placed around the fuselage with 235 points in the streamwise direction and 129 points in the cross-section, as shown in figure 3a. This structure permits the removal of sections along the wing where other topologies can be used to enhance grid resolution, identified in purple shading in figure 3. For each change in topology a decoupling of grid density is introduced. Since a wing is typically modeled with a C-grid topology, the middle section of the O-grid that extends along the side of the shuttle is replaced with a C-grid, as shown in figure 3b. Additionally the tail grid is spanwise mapped with a C-grid. The C-grid on the wing has an additional 48 cells on the upper and lower surfaces for a total of 129 points on the wing, and 225 points in the cross-section that includes the fuselage. The additional 48 cells on the leeside and windside of the wing are enabled through the decoupling provided by the C-grid along the purple topology lines in figure 3b. The dimension along the purple lines is completely independent of all other grid dimensions. The C-grid on the tail places 49 points vertically along the leading edge, without adding more points in the streamwise direction. Thus, enhanced grid resolution of the wing surfaces is enabled through the addition of different topologies.

When the damage scenarios are modeled, the yellow region of figure 1 is replaced with an O-grid because grid density from the edges of the C-grid that connect to the edges of the damage geometry is independent of the remaining sections of the volume grid.

The remaining dimension in this volume grid is the body to outer boundary direction, which was modeled with 65 points. However, if further resolution is required in the boundary layer or bow shock region, this dimension could be easily increased because it is consistent among all the blocks of the common baseline volume grid.

Thus, using a different topology to model different geometric features of the Shuttle Orbiter while maintaining a consistent computational direction for the boundary layer, grid density was enhanced without requiring additional points in regions were the grid resolution was adequate for the accurate capture of flow field phenomenon by the CFD codes.

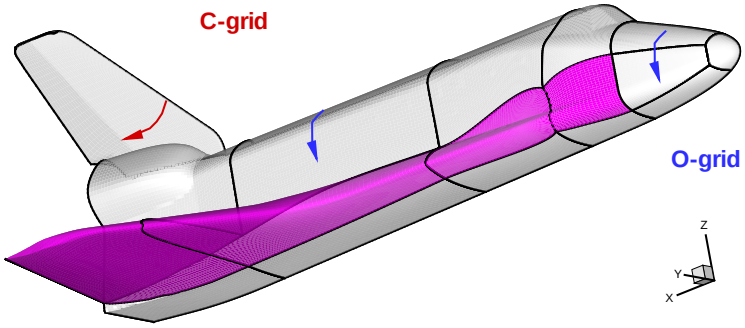

(a) O-grid.

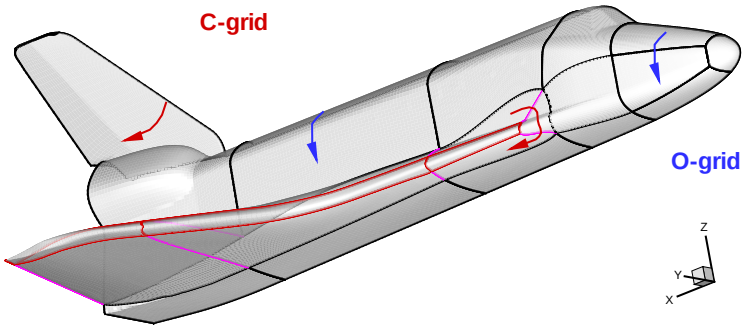

(b) O-C-grid.

Figure 3. Orbiter topology construction.

C. Grid Quality

Most flow simulation software will work with any structured grid, providing the computed cell volumes are always positive. In order to obtain accurate flow simulations, however, very specific conditions of the grid must be met. As noted in the sections above, there are physical characteristics which must exist, such as orthogonality. The most common method of determining the applicability of a grid towards accurate flow simulations is to measure the physical characteristics, also known as grid metrics.

The grid quality metrics used to assess the grids generated for use by the ACAI team were based on extensive experience at NASA Langley Research Center (LaRC) in grid generation. These grid metrics include cell-to-cell stretching, interior and near wall orthogonality, and cell volume. Based on previous work in structured grid generation, grids tangent to the wall should have a stretching less than a factor of 1.5.[5,6] During the ACAI analyses a more stringent requirement of monotonic grid stretching variation was required by the USA software to obtain accurate heating analyses. Grid line intersection within the volume and near the wall of the vehicle should be less than 10 degrees from an orthogonal condition[7] for the grid to be considered to be of high quality. Specific measures are presented later for the family of grids generated.

These metrics were used to assess the grid quality by evaluating the maximum stretching, minimum orthogonality, and root mean square (RMS) values of the orthogonality and stretching. The RMS values were evaluated in combination with a factor of three times the standard deviation to identify the limits of the metrics. Most grids that did not adhere to these metrics were either re-constructed or modified until the

metric limits were satisfied. Based on anecdotal evidence obtained during the use of the grids generated for this investigation, failure to adhere to limits of these metrics can result in inaccurate flow simulations and can slow the convergence of flow field residuals towards an equilibrium state with CFD software.

D. The Process

The build-up of structured grid topologies shown in figure 1 was chosen for the following reasons:

[1] There would be no singularity throughout the flow domain.

[2] The embedded O-grid would permit the local re-construction of a section of the grid to accommodate related damage scenarios, without requiring full generation of the configuration.

[3] The embedded O-grid topology focuses grid resolution to the vicinity of the damage where high grid-point resolution is required.

[4] Grid adaptation in the OML surface normal direction remains an option for those solvers that can use it.

[5] Piecewise construction techniques could be used to spread the workload among different participants.

The first and third issues address the accuracy of the flow simulation software, as previously identified. Conversely, the topology choice was made to permit rapid changing of the shuttle orbiter geometry, leading towards a flexible construction process and an adaptable usage of geometry for complex flow field simulation and analyses. Interchangeable geometric usage is derived from the ability to simply swap volume grid components in order to build different shuttle orbiter configurations. For example, isolating the wing from the body with a C-grid enables the switching of damaged wing components with other previously constructed volume grids for new damage scenario analyses. Each of the damage scenarios that were examined by the ACAI team required the meshing of an interior cavity region in addition to the exterior mesh previously discussed. The interior of the cavity region is fitted with either an H-grid or a double O-grid, depending on the damage scenario and flow solver that was in use.

Given these exterior and interior topologies, the grid construction techniques still had to be defined as appropriate for the various CFD solvers. Within the team, JSC provided direction for the types of geometries to be modeled, while NASA Ames Research Center (ARC) and LaRC shared the responsibilities, utilizing the process identified in figure 4. In figure 4 the steps that ARC were responsible for performing are highlighted in blue, while the steps that LaRC performed are shown in red, and combined responsibilities of ARC and LaRC are shown in purple. The surface grid that was used to model the geometry of the Shuttle Orbiter Columbia was generated by ARC. This usually is one of the most time consuming steps in the grid generation process because the grid is restricted to the surface of the vehicle. Conversely, the interfaces of blocks, and the other faces that define a 3D block are less confined and can move freely within the volume with the only requirement being that these surfaces not intersect one another. Thus, generating 3D surfaces in general 3D space as well as the volume grid that fills each block requires approximately the same amount of work as constructing the surface grid because of the number of surfaces to be generated. Hence, the division of work within this process is equal.

During the use of the grid generation process, several hurdles had to be overcome, including:

[1] obtaining an outer mold line (OML) definition of the shuttle orbiter,

[2] generating block interfaces that are orthogonal to the wall of the vehicle,

[3] maintaining C-2 (curvature) continuity across matching block boundaries, and

[4] limiting grid stretching and skewness at the surface and within the volume.

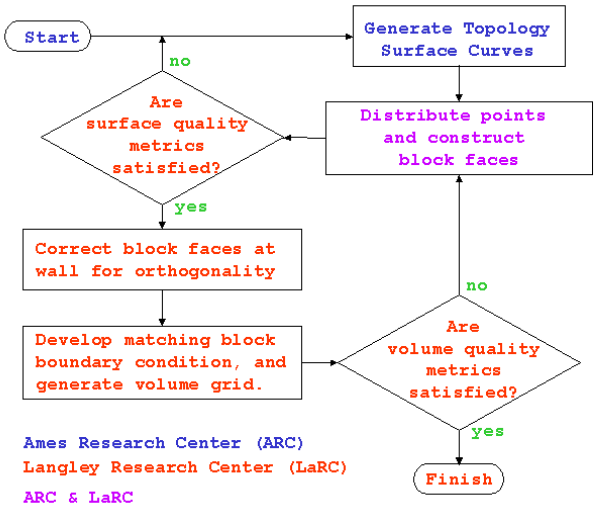

Figure 4. Grid generation process.

Each of these issues are addressed in the following sections. Contained in these sections are also explanations of how the grid generation process unfolded and why the delegation of responsibilities lead to the use of LaRC and ARC resources. This process lead to the successful completion of structured grids for viscous flow simulations in a rapidly developed and high quality product.

IV. Accurate Orbiter Outer Mold Lines

At the time of the Shuttle Orbiter Columbia accident, the most up to date vehicle OML that was available to the ACAI team was that developed by Mississippi State University under contract to JSC in the mid 1990's. Inspection of the surface geometry identified several flaws in wing shape and elevon trailing edge. Hence, a new and more up to date OML was sought. JSC, who had been working on an improved vehicle OML provided this new orbiter definition within the first few weeks of the Columbia accident.

Due to some geometry nuances and minor flaws in the new OML, an effort was undertaken by both ARC and LaRC to construct a "watertight" OML of the shuttle orbiter using two different methods. The method utilized by ARC was designed to obtain an OML shape that could be used to assess aerothermodynamic issues. Only the tail and wing trailing edge regions, which have the most complicated geometry, were slightly modified to ensure that rapid flow simulations could be performed. Specifically, ARC appended small regions of false surfaces to the Orbital Maneuvering System (OMS) pods and the wing to simplify the geometry, as shown in figure 5. Break-lines along the actual geometry were maintained so that subsequent aerodynamic force integration could be performed on solution data obtained during the aerothermodynamic analyses. Geometry was added to close gaps and eliminate abrupt geometry changes which were necessary changes to the OML for structured surface and volume grid generation.

The second watertight OML was developed by LaRC using the new JSC provided geometry, and resulted in a more accurate representation of the orbiter needed for aerodynamic simulations. This OML surface was not used for the ACAI team because the details were too difficult to accommodate with a structured grid. Rather, it was used for unstructured grid generation for performing inviscid flow field simulations. No superfluous surfaces were added, and strong surface discontinuities present in the actual Shuttle OML were

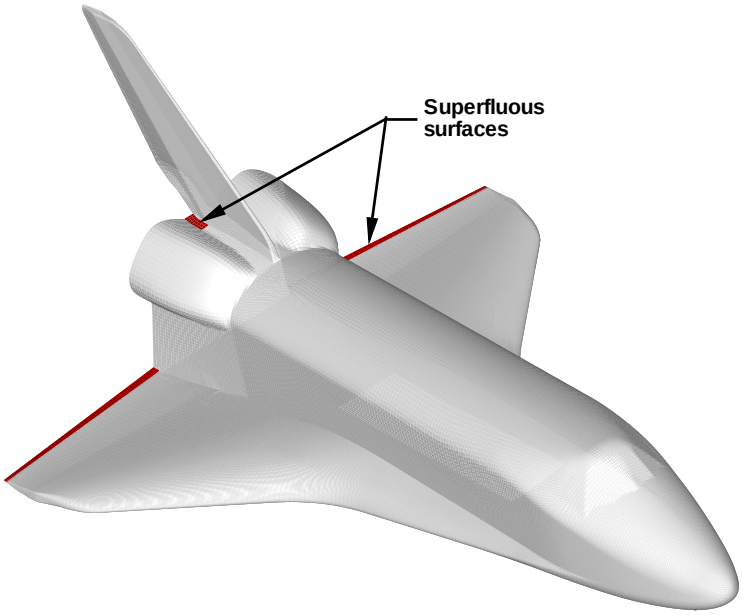

Figure 5. Ames Research Center OML modifications.

maintained. Each OML was used in the investigation, and differed only on the top and trailing edge of the vehicle. Since aerothermodynamic characteristics are not usually influenced by these regions, the differences in geometry were considered negligible.

V. Generating High Quality Grids

With the OML established for aerothermodynamic simulations, the process identified in figure 4 commenced. As noted in figure 1, the topology of the grid was agreed upon prior to generating any grids. During the investigation it became clear that several grids would have to be generated. Although the topology provides a working structure where damage scenarios to the orbiter could be easily accommodated, the detailed local regriding was required to support each specific damage scenario. The GridGen[8] software was used for this portion of the grid construction. Several versions of the wall surface grid were evaluated by LaRC for skewness and stretching during the wall grid generation process. The Tecplot[9] software in conjunction with the CFD Analyzer[10] (CFDA) was used to perform the computations for evaluating grid skewness and stretching. CFDA was chosen because of its integration into the Tecplot environment and because it was able to assess grid stretching across matching block boundaries. Each consecutive grid generated had consistent increasing quality, as the skewness and stretching was minimized.

A. Block Interface Orthogonality Enhancement

Once the wall grid was complete, the volume grid construction commenced. This portion of the process was performed by ARC and LaRC in concert with one another. Due to the construction techniques available, controlling the block interfaces at the wall of the orbiter was very difficult. Although the GridGen software does have the ability to project grid lines orthogonal to the wall, generating the entire interface with an edge

along the wall surface such that the interior grid of the interface is orthogonal to the wall, is impossible. There exists no method within GridGen to ensure that the interface grid along the wall of the Orbiter is orthogonal. Hence, an alternative technique had to be used.

Through extensive work at LaRC on the X-37 program, a method to improve an existing surface grid for orthogonality was developed. This technique, requires an initial surface grid and the vectors to control the location of the grid along an edge. The vectors, typically obtained from the CFDA, are combined with the initial surface grid in the Volume Grid Manipulator[11] (VGM) tool to produce an orthogonally corrected interface. Briefly, referring to figure 6 for vector construction and figure 7 for the corrected grid, the method entails the following steps:

[1] Input the initial surface grid and the controlling vectors along an edge.

[2] Reverse the controlling vectors along an edge.

[3] Construct a second set of vectors interior to the interface grid, but close to the edge where corrections are to be performed.

[4] Utilize Hermite Vector Interpolation[12] (HVI) to regenerate a region close to the edge in question by interpolating the vector fields.

[5] Perform Trans-Finite Interpolation[13] on a small region near the ends of the modified edge grid.

[6] Output the corrected grid for elliptic smoothing.

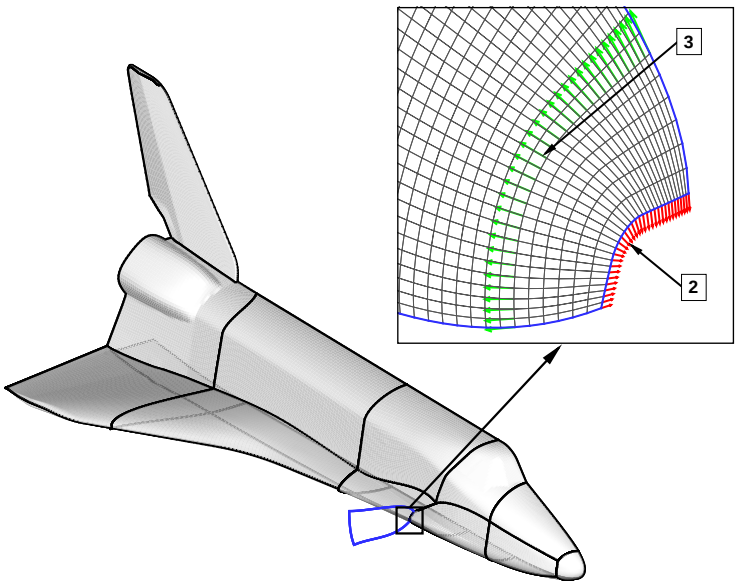

Figure 6. Vectors used within VGM to correct orthogonality of a block interface grid near the wall.

The resulting grid, as shown in figure 7 is orthogonal to the wall based on the adherence to the vector field used to create it. This VGM created surface grid is then used as a defining surface within GridGen, to construct a new surface mesh. A final surface grid is created by elliptically smoothing the new surface mesh within GridGen using both wall orthogonality and a fixed surface condition to ensure both orthogonality to the OML and orthogonality to the surface grid edges. Each interface connected to the wall is corrected in the same manner with the VGM software. This correction ensures that the volume grid based on these interfaces can be orthogonal to the wall of the orbiter, thus satisfying a desired grid attribute for the CFD

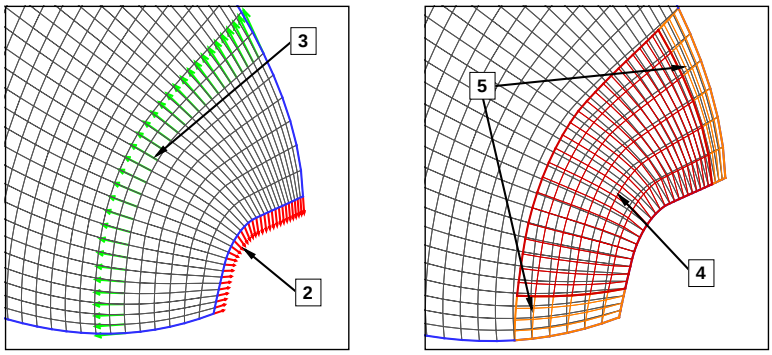

Figure 7. Corrected block interface grid near the wall using HVI and TFI.

solvers. Additionally, by manipulating the grid in VGM, the process is fast and efficient, so rapid generation of the volume grid is not impeded.

B. Imposing C-2 Continuity While Limiting Skewness and Stretching

Upon completion of generating and correcting the interfaces of the volume grid to be constructed, the volume grid is generated. Volume grid generation for the Shuttle Orbiter was performed primarily using GridGen and 3DGRAPE/AL[14] when GridGen failed. In particular, the topology of the tail region was implemented using complex surface grids which made it extremely difficult for GridGen to generate a grid without crossed grid lines. As such, this region was generated with the 3DGRAPE/AL software. The most difficult issue to overcome in the volume grid generation was the construction of continuous grid lines across matching block boundaries. Typically, software such as GridGen uses an orthogonal grid condition across such a boundary. Although this does produce a continuous grid line across the matching block interface, the resulting grid is difficult to control on the interior of the domain, and inflections in the grid can lead to excessive skewness of the mesh within the volume domain. There are several methods for producing slope continuous grid lines across matching block boundaries, but each has disadvantages that are not conducive to rapid structured volume grid generation. For example, use of a Neumann boundary condition or averaging the point locations at the first cell away from the interface will change the interface entirely. Another technique is to swap the vectors from one block into the other that share an interface. The latter method is used by GridGen and can require multiple exchanges of angles across a matching block interface before the slope continuous grid line is produced. Regardless of the method used, to date there has been no boundary condition that will preserve the interface and provide slope continuous grid lines across matching block interfaces for rapid volume grid generation.

To overcome the problems associated with the development of slope continuous grid lines across matching block boundaries, a new technique to correct the grid was developed specifically for the ACAI. The method makes use of vector field averaging. The steps involved include:

[1] Computing vector fields from the first cell away from the interface on both sides or in each block that share the interface.

[2] Reversing one vector field from one side of the interface.

[3] Averaging the vectors at the interface.

[4] Reversing a copy of the vectors to the side where the vectors from step 2 originated.

[5] Using the vectors to project the first cell points to correct the first layer of grid away from the interface in both blocks that share the interface.

The steps above perform the correction. However, to use the correction effectively, the correction has to be performed several times. As shown in figure 8a with a representative plane from a volume grid on the Orbiter, the grid is initially generated with 3DTFI. Then the correction is applied as shown in figure 8b, and the volume grid is smoothed again, but maintaining the angles and cell sizes produced from the correction at the interface, resulting in the grid shown in figure 8c. This cycle of smoothing and correcting is performed 2 to 3 times in order to obtain the slope continuous condition across the matching block interface. The result of using this method is a high fidelity structured volume grid with slope continuous grid lines across all matching block interfaces.

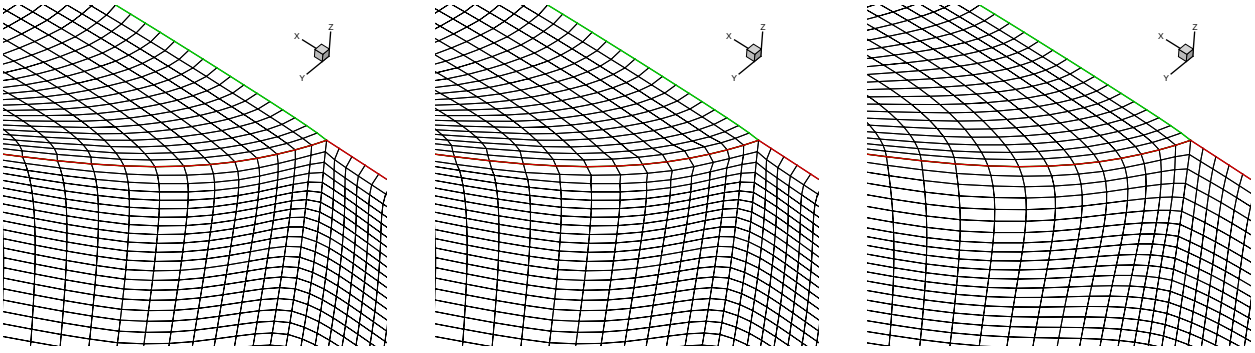

(a) Initial grid. (b) Corrected interface. (c) Smoothed correction.

Figure 8. A single cycle for applying the matching block interface continuity correction.

VI. Grids Generated and Quality

A. Wall Surface Grids

Utilization of the grid generation process with the new technology and the teamwork resulted in a rapid generation of surface and volume grids. The first mesh was generated using the flexible framework process for the baseline undamaged configuration shown in figure 1. This first volume grid required approximately eight weeks to build. The vast majority of problems related to mesh defects such as grid stretching and grid line intersection skewness, and data transfer problems between LaRC and ARC were discussed and resolved using this first mesh. For example, the initial surface mesh generated by ARC and analyzed by LaRC had poor stretching and boundary matching parameters. In order to determine the applicability of the surface grid for volume grid generation, a new structured grid generation parameter[15] called GQ was used to assess the combined effects of grid stretching and grid orthogonality on the wall. The GQ measure is given by

$$GQ = \frac{\theta_\zeta}{\nabla^2 \vec{r}_{\xi,\eta}} \Theta \tag{1}$$

The original form of the GQ measure includes a straightness measure, Θ, but for surface grids this measure is set to one to remove its dependency. Grid stretching is evaluated for both directions by using equations

$$\nabla^2 \vec{r}_\xi = \frac{\max\left(|\vec{r}_\xi|^+, |\vec{r}_\xi|^-\right)}{\min\left(|\vec{r}_\xi|^+, |\vec{r}_\xi|^-\right)} \tag{2a}$$

$$\nabla^2 \vec{r}_\eta = \frac{\max\left(|\vec{r}_\eta|^+, |\vec{r}_\eta|^-\right)}{\min\left(|\vec{r}_\eta|^+, |\vec{r}_\eta|^-\right)} \tag{2b}$$

The grid orthogonality is determined by the percentage of an orthogonal intersection given by equation

$$\theta\,|_{\zeta=constant} = \frac{2}{\pi}\cos^{-1}\left(\frac{\left|\vec{r}_\xi \cdot \vec{r}_\eta\right|}{|\vec{r}_\xi||\vec{r}_\eta|}\right) \tag{3}$$

For both the grid stretching and grid orthogonality, the best measure is unity, while the worst grid stretching is infinite and the worst grid orthogonality is zero. Hence, the best possible measure is one, while values less than one are of decreasing quality. By combining the orthogonality and stretching measures in the form shown in equation 1, the GQ will vary from 0 indicating extremely poor quality, to 1 for the best quality. Utilizing the grid stretching, orthogonality, and the GQ measure, the progression of the wall grid construction is shown in figure 9, and tabulated in tables 1.

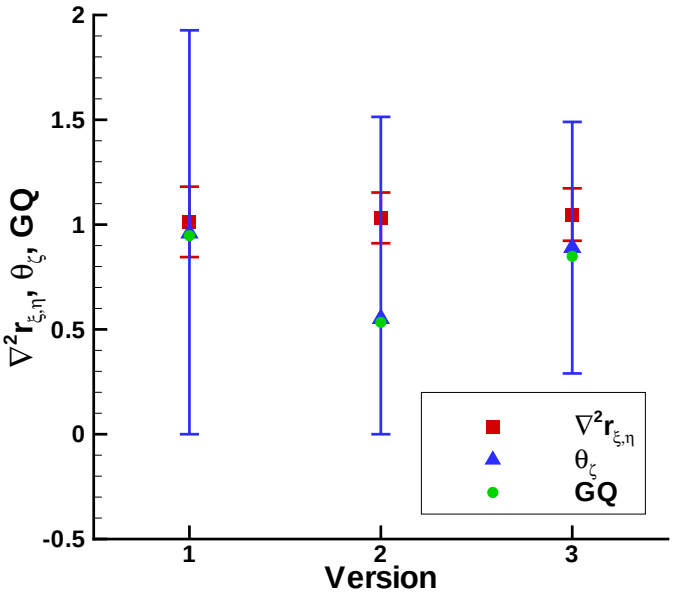

Figure 9. Grid quality assessment through the progression of wall surface grid generation. (Error bars are 3σ deviations.)

The GQ measure does not have a variation that is easily determined because the distributions of the stretching and orthogonality are non-Gaussian. Assessment of the initial surface grid generated by ARC indicated significant deviations in grid quality, evidenced by large 3σ values of grid stretching and orthogonality. Through the feedback loop and grid quality analyses, the grid quality improved through the tracking of the 3σ values of the grid metrics. The second grid produced indicated significant grid skewness but improvements to the variation in the quality measures. The third and final common baseline wall surface grid was of good quality, and was used in the development of the volume grid used for the ACAI because the variation in the component grid metrics was smaller than previously generated grids, and the GQ measure was closer to unity.

Table 1. Grid stretching, orthogonality, and quality metric data for wall surface grid generation.

Ver.	$\max\left(\overline{\nabla^2 \vec{r}_{\xi,\eta}}\right)$	$\pm 3\sigma_{\xi,\eta}$	$\max\left(\overline{\theta_\zeta}\right)$	$\pm 3\sigma_\zeta$	GQ
1	1.013	0.168	0.959	0.968	0.947
2	1.032	0.121	0.551	0.963	0.534
3	1.048	0.125	0.890	0.600	0.849

Upon completion of the baseline common grid, the process had matured to the extent that subsequent grids where damage was included were generated efficiently with very few iterations required to obtain the desirable quality. To evaluate flow conditions and phenomenon related to the ACAI, four full body exterior damage scenario volume grids were generated using the established process in figure 4. Each grid was generated by removing the yellow region in figure 1, and regenerating the region to reflect the different damage scenarios, including those shown in figure 10. These new regions were inserted back into the baseline common mesh to produce a new volume grid. Hence, the damage grid regions were interchangeable.

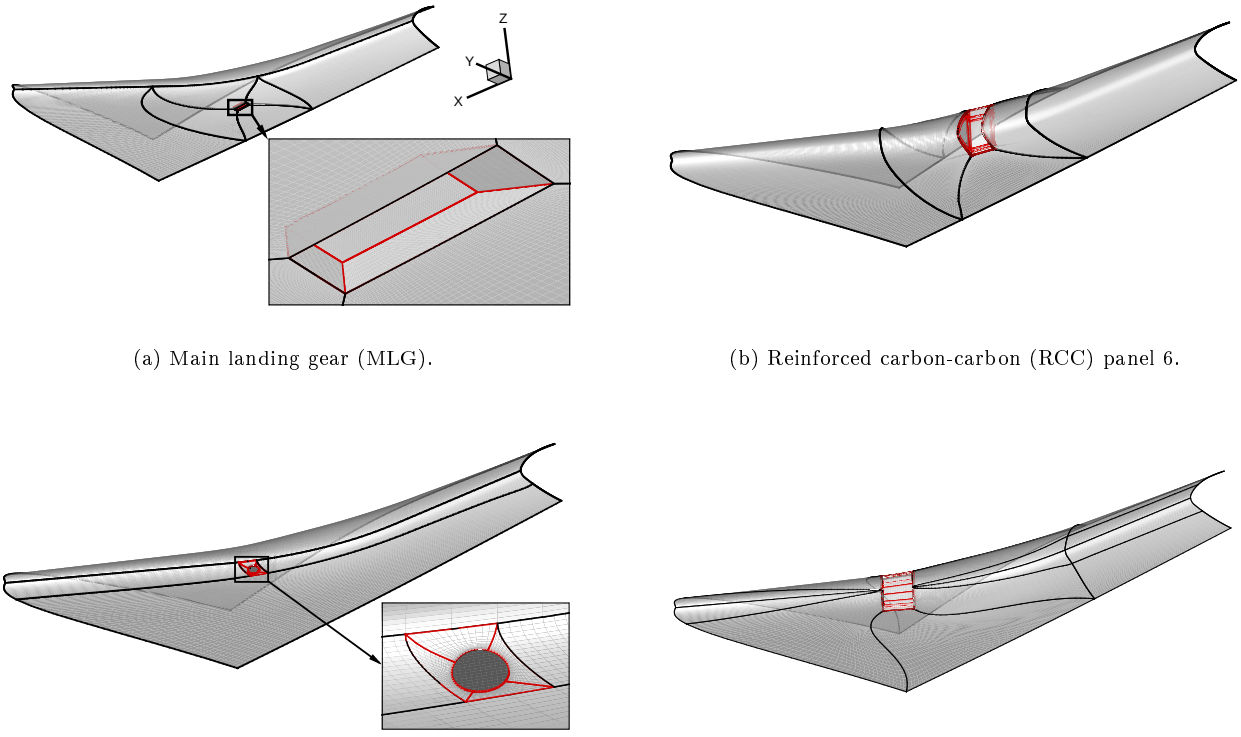

(a) Main landing gear (MLG).

(b) Reinforced carbon-carbon (RCC) panel 6.

(c) Reinforced carbon-carbon (RCC) panel 8.

(d) Reinforced carbon-carbon (RCC) panel 9.

Figure 10. Four damage scenario surface geometries and topologies for the aerothermodynamic simulations of the ACAI.

In each of the geometries shown in figure 10, cavities were generated and inserted where the red topology lines are drawn. For the RCC Panel 6 and 9 cases, multiple cavity grid topologies were developed for half

and full panel missing configurations, but each used the same exterior surface and volume mesh. In each cavity case the inner face of the exterior volume mesh in the region directly above the intended cavity was developed to correspond to the original OML surface.

B. Volume Grids

The baseline volume grid was generated using the standard techniques available with GridGen, 3DGRAPE/AL, and VGM. It was based entirely on the ARC generated wall and interface surface grids with corrections from LaRC. Representative representative planes for this baseline grid are shown in figure 11, with grid quality metrics listed in table 2.

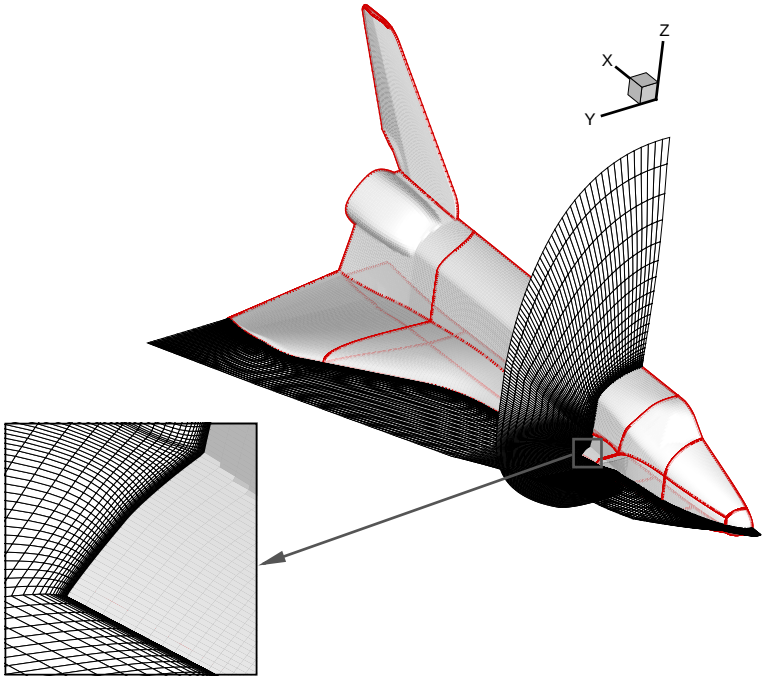

Figure 11. Baseline common mesh with representative planes for volume visualization.

Table 2. Baseline common grid quality measures.

Metric	Minimum	Mean $\pm 3\sigma$	Maximum
$\nabla^2 \vec{r}_\xi$	1.000	1.049 ± 0.131	2.017
$\nabla^2 \vec{r}_\eta$	1.000	1.011 ± 0.145	2.142
$\nabla^2 \vec{r}_\zeta$	1.000	1.148 ± 0.217	1.678
θ_ξ	0.018	0.903 ± 0.751	1.000
θ_η	0.042	0.930 ± 0.533	1.000
θ_ζ	0.023	0.877 ± 0.568	1.000
ϕ_ζ	0.000	0.012 ± 0.301	0.891

Although the maximum grid stretching exceeded the target of 1.5, the time-line requirements of the accident investigation did not allow for further refinement. Refinement was warranted but not pursued so that the assessment of damage scenarios could start. The baseline common volume grid required approximately eight weeks to complete, which represents a significant time savings by a factor of 50%; typical volume grids of this nature require ten to twelve weeks to generate. The addition of the block interface correction and slope continuity condition technologies were the primary contributing factors to this reduction in time.

For boundary layer modeling accuracy the correction to the block interfaces was crucial. The last measure in table 2 measures the extent of grid orthogonality with respect to the local unit normal vector at the wall, and is computed using

$$\phi_\zeta = \frac{2}{\pi}\cos^{-1}\left(\frac{\left|\vec{r}_\zeta \cdot \vec{r}_{\hat{n}}\right|}{|\vec{r}_\zeta||\vec{r}_{\hat{n}}|}\right) \tag{4}$$

The angle measurement is best at zero and worst at the maximum. This measure is one that is easier to evaluate pictorially than through the measurement because it is a local property to the wall. Illustrated in figure 12, the near wall orthogonality measurement indicates a maximum deviation of 80 degrees which occurs at the tail leading edge, a region of difficult grid construction due to topology and available controls for grid generation.

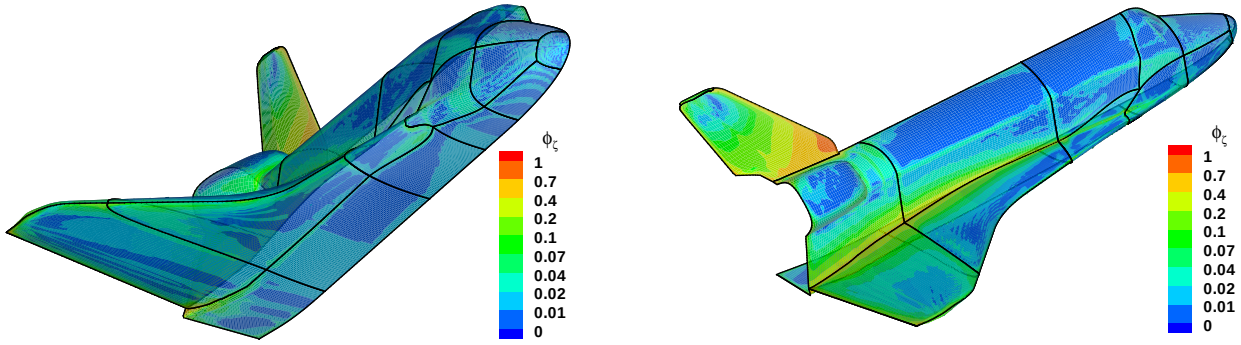

(a) Wind side.

(b) Lee side.

Figure 12. Wall orthogonality with respect to local unit normals.

The mean of the orthogonality measure at the wall is 1 degree, which corresponds to a value of $\phi = 0.012$, indicating that the block boundary corrections have a measurable impact. Original angles at the block interfaces were between 30 to 50 degrees from the wall unit normals. Hence, using the corrections to the block interfaces should promote improved boundary layer modeling with the baseline common volume grid. The GQ measure given by

$$GQ = \frac{\overline{\theta_{\xi,\eta,\zeta}|_{min}}}{\nabla^2 \vec{r}_{\xi,\eta,\zeta}|_{max}}\Theta \tag{5}$$

for this volume grid is 0.759, which is moderate based on the trends established for this measure in 3D.[15] Initially, the GQ measure was used as a filter of good and bad grids. But in the current work, the variation of component measures identified that large values of GQ could have significant variations. The histograms of the component measures indicate non-Gaussian distributions, where the mean is shifted to one side of the histogram. With this type of variation and distribution of the components to the GQ measure, there appeared to be no simple method of determining the variations of the GQ measure. Hence, the best grid is considered to be the highest GQ with the lowest variation of component measures.

During the use of the baseline common volume grid several issues arose, including skewness sensitivities in the tail region for the GASP software, stretching sensitivities in the boundary layer for the USA code, and adaptability with the LAURA code. Each ACAI member site had issues with this volume grid, but were able to overcome them nonetheless. Although there was no clear analytical method to identify the root causes of the problems with respect to grid quality, the GQ measure remains an indicator of usable grid data, and the range of 0.70-0.80 indicates questionable usage issues, evident by the ACAI team's feedback.

As noted earlier, the remaining families of volume grids based on the surface geometries illustrated in figure 10 were constructed by removing the shaded yellow region of figure 1. The grid quality metrics for these volume grids are listed in order of appearance in figure 10, in tables 3.

Table 3. Grid quality measures for four different types of damage scenario volume grids.

Metric	Minimum	Mean $\pm 3\sigma$	Maximum
$\nabla^2\vec{r}_\xi$	1.000	1.023 ± 0.125	2.017
$\nabla^2\vec{r}_\eta$	1.000	1.012 ± 0.139	2.142
$\nabla^2\vec{r}_\zeta$	1.000	1.141 ± 0.215	1.678
θ_ξ	0.018	0.964 ± 0.912	1.000
θ_η	0.042	0.989 ± 0.546	1.000
θ_ζ	0.023	0.816 ± 0.648	1.000
ϕ_ζ	0.000	0.026 ± 0.244	0.891

(a) Damaged main landing gear door grid quality measures, with GQ=0.713.

Metric	Minimum	Mean $\pm 3\sigma$	Maximum
$\nabla^2\vec{r}_\xi$	1.000	1.034 ± 0.200	2.017
$\nabla^2\vec{r}_\eta$	1.000	1.020 ± 0.179	2.142
$\nabla^2\vec{r}_\zeta$	1.000	1.021 ± 0.270	1.678
θ_ξ	0.018	0.602 ± 0.754	1.000
θ_η	0.042	0.895 ± 0.759	1.000
θ_ζ	0.023	0.869 ± 0.670	1.000
ϕ_ζ	0.000	0.089 ± 0.245	0.891

(b) Missing RCC panel 6 grid quality measures, with GQ=0.577.

Metric	Minimum	Mean $\pm 3\sigma$	Maximum
$\nabla^2\vec{r}_\xi$	1.000	1.070 ± 0.297	5.987
$\nabla^2\vec{r}_\eta$	1.000	1.033 ± 0.272	3.899
$\nabla^2\vec{r}_\zeta$	1.000	1.118 ± 0.243	7.569
θ_ξ	0.018	0.892 ± 0.792	1.000
θ_η	0.042	0.847 ± 0.555	1.000
θ_ζ	0.023	0.805 ± 0.603	1.000
ϕ_ζ	0.000	0.238 ± 0.311	0.891

(c) Damaged RCC panel 8 grid quality measures, with GQ=0.715.

Metric	Minimum	Mean $\pm 3\sigma$	Maximum
$\nabla^2\vec{r}_\xi$	1.000	1.029 ± 0.426	2.170
$\nabla^2\vec{r}_\eta$	1.000	1.038 ± 0.352	2.142
$\nabla^2\vec{r}_\zeta$	1.000	1.191 ± 0.262	1.821
θ_ξ	0.000	0.794 ± 0.675	1.000
θ_η	0.042	0.954 ± 0.419	1.000
θ_ζ	0.023	0.916 ± 0.566	1.000
ϕ_ζ	0.000	0.057 ± 0.269	0.891

(d) Missing RCC panel 9 grid quality measures, with GQ=0.662.

By comparison to the baseline common volume grid, similar flow solver issues arose with the volume grids for the missing RCC panels 6 and 9. The GQ measure clearly indicated which grids would be difficult to use and which may cause minor issues. However, the fast pace of performing CFD and the need to obtain credible data in a short time frame prevented further modification of these volume grids for enhanced usability.

After the completion of the baseline grid, subsequent surfaces and volume grids for the damage scenarios were built. The volume grids constructed for the damage scenarios were only built for the region described by the surfaces in figure 10, and they made use of the interfaces within the baseline common grid. This construction technique resulted in a set of four interchangeable volume grids. Due to the interchangeability of these damage scenarios, the bulk of the surface and volume grids did not have to be rebuilt. The process in place for grid generation set into motion an assembly line method for grid generation. While ARC was generating surface grids, LaRC was generating volume grids. Utilizing the assembly line approach and re-using existing volume grid data, a time savings of six weeks resulted because each scenario only required an average of two weeks to generate. Hence, nearly 24 weeks of work was saved using the flexible framework and a division of labor for grid generation with the new construction technologies.

In most cases the interior cavity grids were constructed by the individual organizations responsible for calculating the particular damage scenario case. All cavities, except RCC-8, were modeled with various boundary conditions to simulate a pressurization of the wing leading edge. Only RCC-8 had an interior volume grid that extended beyond the cavity itself and included a portion of the channel of the wing leading edge. By limiting the scope of the volume grid generation to the specific damage scenario location, resources were focused on the generation of high fidelity grids for the region of the wing leading edge. This significantly reduced the time required to assemble a new full body volume grid because the wing leading edge region was simply swapped for the different grids. Note that in some cases, the grid density was modified along the fuselage blocks to enable finer grid resolution in the cavities to be modeled. Nonetheless, the process used and the limiting of scope of the grid generation enabled rapid volume grid generation for the ACAI.

VII. Summary

A flexible framework for the generation of high fidelity structured volume grids for use with the Columbia Accident Investigation (CAI) was developed. The framework consisted of a grid generation process and a division of labor among the aerothermodynamic CAI team members. The process was a compromise between grid generation time and grid quality, given the the aggressive time-line and wide range of flow solver capabilities. Given more time, other best practices in grid generation, such as topology refinement and elliptic smoother source term combinations, could have been utilized. The topologies utilized in this framework for damage scenario grids was the embedded O-grid, which enables grid metric customization with respect to the geometry alteration without adversely affecting grid requirements on the remainder of the vehicle. The embedded O-grid topology also permitted the construction of multiple geometric changes through the regeneration of a limited, focused region of the baseline volume grid. The process utilized the strengths of decoupled surface and volume grid generation with constant evaluation of grid quality, to ensure that the final grid for computational use would be acceptable to all participants in the aerothermodynamic computations of the CAI. Utilizing an assembly line approach with a combination of teamwork between NASA Centers and the grid generation process, high fidelity grids were generated rapidly for the ACAI.

References

[1]P. A. Gnoffo, "An Upwind–Biased Point–Implicit Relaxation Algorithm for Viscous, Compressible Perfect–Gas Flows," NASA Technical Paper 2953, February 1990.

[2]R. W. Walters, D. C. Slack, P. Cinnella, M. Applebaum, and C. Frost, *GASP Version 3, The General Aerodynamic Simulation Program, Computational Flow Analysis Software for the Scientist and Engineer, User's Manual*. Blacksburg, VA: Aerosoft Incorporated, 1st ed., May 1996.

[3]S. R. Chakravarthy and S. Osher, "Computing with high-resolution upwind schemes for hyperbolic equations," in *Proceedings of the 1983 AMS-SIAM Summer Seminar on Large-Scale Computations in Fluid Mechanics*, vol. 22, American Mathematical Society in Lectures in Applied Mathematics, 1985.

[4]C. C. Wong, M. Soetrisno, F. G. Blottner, S. T. Imlay, and Payne, "PINCA:A Scalable Parallel Program for Compressible Gas Dynamics with Nonequilibrium Chemistry," Sandia National Laboratories Report SAND 94-2436, 1995.

[5]D. R. Olynick, "Importance of 3–D Grid Resolution and Structure for Calculating Reentry Heating Environments," AIAA Paper 96–1857, June 1996.

[6]W. Z. Strang, "QBERT: A Grid Evaluation Code," AFWAL Technical Memorandum 99–193, Wright Research and Development Center Report, July 1988.

[7]J. F. Thompson, Z. U. A. Warsi, and C. W. Mastin, *Numerical Grid Generation: Fundations and Applications.* New York, New York: North-Holland, 1st ed., 1985.

[8]J. P. Steinbrenner, J. R. Chawner, and C. L. Fouts, "The GRIDGEN 3D Multiple Block Grid Generation System," Wright Research and Development Center Report TR–90–3022, July 1990.

[9]Amtec Engineering Inc., "Tecplot: version 9 User's Manual," Amtec Engineering publication V9.0/2001, August 2001.

[10]Amtec Engineering Inc., "CFD Analyzer^{TM} 3.0: User's Manual," Amtec Engineering publication V3.0/2002, June 2002.

[11]S. J. Alter, *The Volume Grid Manipulator (VGM): A Grid Reusability Tool.* No. 4772, NASA Contractor Report, April 1997.

[12]S. J. Alter, *The Volume Grid Manipulator (VGM): A Grid Reusability Tool*, ch. 9, pp. 78–82. No. 4772, NASA Contractor Report, April 1997.

[13]W. J. Gordon and C. A. Hall, "Construction of Curvilinear Coordinate Systems and Applications to Mesh Generation," *International Journal of Numerical Methods in Engineering*, vol. 3, pp. 461–477, July 1973.

[14]S. J. Alter, "Efficient Development of High Fidelity Structured Volume Grids for Hypersonic Flow Simulations," AIAA Paper 2003–0952, January 2003.

[15]S. J. Alter, "A Structured-Grid Quality Measure for Simulated Hypersonic Flows," AIAA Paper 2004–0612, January 2004.